FUDMA Journal of Engineering and Technology
ISSN: 3092-9385
https://fjet.fudutsinma.edu.ng/index.php/fjet/
Volume 2, Issue 2, 2026, 303-313

DSAF-Net: A Dynamic Scale-Aware Attention Fusion Network for Multiclass Brain Tumour Classification from MRI Images

Oluwadare A. ADEBISI[1*], Ibiyemi I. ADEAGA[2], Samson O. AYANLADE[3], Khadijah O. LAWAL[4]

[1] Department of Electrical and Electronics Engineering, Bowen University, College of Agriculture, Engineering, and Science, Iwo, Nigeria
[2] Department of Computer Engineering, The Polytechnic Ibadan, Nigeria
[3]Department of Electrical and Electronics Engineering, College of Engineering and Environmental Studies, Olabisi Onabanjo University, Ago-Iwoye, Nigeria
[4]Department of Mechatronics Engineering, Abiola Ajimobi Technical University, Ibadan, Nigeria

[1*]oluwadare.adebisi@bowen.edu.ng, [2]mummyajibo@gmail.com, [3]ayanlade.oladayo@oouagoiwoye.edu.ng, [4]khadijah.lawal@tech-u.edu.ng

Abstract
Accurate classification of brain tumours from magnetic resonance imaging (MRI) plays a crucial role in early diagnosis, treatment planning, and clinical decision-making. Although deep learning approaches have advanced automated tumour analysis, many existing models remain constrained by inadequate feature representation, loss of discriminative information, inconsistent generalisation, and growing computational demands. Addressing these challenges requires learning frameworks capable of capturing heterogeneous tumour characteristics while maintaining practical computational efficiency. This study presents a Dynamic Scale-Aware Attention Fusion Network (DSAF-Net) for multiclass brain tumour classification from MRI images. The proposed architecture integrates residual multi-scale feature extraction, Dynamic Scale-Aware Attention Fusion modules, hybrid spatial-channel attention, and cross-scale feature fusion within a unified framework. Through adaptive weighting and aggregation of complementary feature representations across multiple receptive fields and network depths, the model enhances discriminative feature learning while preserving computational efficiency. Evaluation was conducted using 4,400 MRI images obtained from Kaggle. The proposed framework achieved an accuracy of 98.94%, precision of 98.87%, recall of 98.76%, F1-score of 98.81%, and an area under the receiver operating characteristic curve (AUC) of 99.72%. Comparative analysis demonstrated consistent performance improvements over SqueezeNet, DenseNet121, and EfficientNet-B7. By combining high predictive accuracy with computational practicality, the proposed framework offers a promising direction for the development of adaptive multi-scale attention-based solutions in medical image analysis.

Keywords: *Brain Tumor Classification; Magnetic Resonance Imaging (MRI); Dynamic Scale-Aware Attention Fusion Network; Multi-Scale Feature Learning; Cross-Scale Feature Fusion; Medical Image Analysis.*

1.0 Introduction

Brain tumours are critical medical conditions that require early and accurate diagnosis for effective treatment planning [1]. Brain tumours constitute a significant medical challenge worldwide, with their classification being critical for timely and efficient intervention [2]. Medical imaging is crucial for diagnosing and categorising brain tumours [3]–[5]. However, radiologists must devote much time and are prone to human error while manually interpreting these images [6], [7]. The study of medical image processing has been completely transformed by deep learning, particularly Convolutional Neural Network (CNN) [8], [9]. CNNs are excellent for functions like tumour classification because they can automatically extract hierarchical information from images [10], [11]. These networks recognise complex patterns and structures in medical images that might be challenging for human observers [12], [13]. Deep learning, a branch of artificial intelligence, has shown remarkable potential in automating the analysis of medical images, including the classification of brain tumours [14]–[16]. This allows for precise and effective classification of brain tumour images, improving early diagnosis and treatment planning in neuro-oncology. Specific forms of brain tumours can be reliably identified and categorised from picture data using CNNs and other deep learning architectures [17], [18].

A deep learning model for brain tumour classification must be trained on a collection of labelled brain images [19]. This dataset should include images containing different types and sizes of tumours and regular brain scans for contrast [20]. Proper data preprocessing techniques ensure uniformity and consistency in the dataset, including resizing images and normalisation [19], [21]. The architecture of the deep learning model is crucial for the accuracy of brain tumour classification [14]. Two-Dimension (2D) or Three-Dimension (3D) CNN architectures are typically employed [9]. Researchers may choose established architectures or design custom models. Transfer learning, where a pre-trained model (e.g., ResNet, Inception) is fine-tuned on medical images, can also be a practical approach, especially where few datasets are available [12], [22].

Received: 04/07/2026; Revised:13/07/2026; Accepted: 16/07/2026; Published: 21/08/2026

Training, validation, and test sets are created from the labelled dataset to develop an automated diagnosis system for brain tumour identification [23]. The validation set monitors the model's performance, and the training set serves to train the model [24]. Evaluation metrics are employed to assess the effectiveness of the model on the test set [17], [18], [25]. A successfully trained deep learning model that can be integrated into clinical practice as a decision-support system [26]. Radiologists can use the model's predictions to assist in diagnosis and treatment planning, ultimately improving patient outcomes.

Despite the considerable advances achieved by deep learning and CNN-based methods for brain tumour classification, several limitations continue to hinder their widespread clinical adoption. Many existing approaches experience inadequate feature representation and the loss of discriminative information during deep feature extraction, which can reduce their ability to distinguish between tumour subtypes accurately [27]. Furthermore, the reliance on individual network architectures often limits the capture of complementary image characteristics, while issues related to class imbalance, poor generalisation across tumour categories, and high computational complexity remain insufficiently addressed. These shortcomings frequently result in inconsistent classification performance and reduced robustness when applied to diverse clinical datasets. Therefore, there is a need for a more effective and computationally efficient framework capable of learning richer and more discriminative representations from brain MRI images. To address these challenges, this study proposes a novel deep learning framework for multiclass brain tumour classification. The main contributions of this work are as follows:

(1) Development of an enhanced classification framework that improves feature extraction and representation learning from brain MRI images

(2) Integration of complementary discriminative features to strengthen tumour class differentiation and improve classification reliability across multiple tumour categories

(3) Design and comprehensive evaluation of a computationally efficient model that achieves high classification performance while maintaining practical suitability for clinical decision-support applications.

2.0 Related work

The comparative study of custom CNNs for enhanced brain tumour detection is a critical area of research, particularly given the increasing reliance on advanced imaging techniques such as MRI. Integrating deep learning methodologies, specifically CNNs, has shown significant promise in improving brain tumour detection and classification accuracy and efficiency. This synthesis will explore the current state of research, highlighting key findings and methodologies from various studies. Recent studies have demonstrated the effectiveness of various CNN architectures tailored for brain tumour detection. For instance, [28] emphasises the need for a simplified network architecture that can operate in real-time during surgical procedures, suggesting that adapting CNNs for 3D imaging could enhance tumour localisation and classification accuracy. Using deep learning techniques such as CNNs, the detection and classification of brain tumours from MRI images have shown encouraging results. [29] emphasises the role of open-source datasets in facilitating the development of CNN models, with the integration of multimodal MRI data being a focal point in enhancing the robustness of CNNs for brain tumour detection.

The discussion in [30] shows how architectures such as U-Net and DeepMedic have been developed to address challenges like tumour heterogeneity and irregular shapes. The use of multiple MRI modalities has dramatically increased the accuracy of detection. This multimodal approach enables a more thorough examination of the tumour's characteristics, improving diagnostic results. Numerous investigations have looked into using cutting-edge methods to enhance detection efficiency. For instance, [31] stipulates a deep learning model incorporated into an approachable online application, showcasing the potential for automated diagnosis in clinical settings. Furthermore, the work by [32] illustrates the effectiveness of a multimodal deep learning strategy that improves segmentation accuracy and overall detection performance by combining several MRI sequences.

Despite the advancements, challenges remain in deploying CNNs for brain tumour detection. Significant hurdles include the need for extensive training datasets, potential overfitting, and deep learning models' computational requirements. The study of [33] addresses these challenges by proposing data augmentation techniques to improve model robustness and detection success rates. Future research should focus on optimising CNN architectures to balance accuracy with computational efficiency and exploring the potential of ensemble learning methods to enhance classification performance [34]. These developments are meant to help medical practitioners diagnose and treat brain tumours by creating clinical decision-support systems. However, [35] emphasises combining CNNs with physiological MRI data to create a comprehensive decision-support framework. This integration could facilitate therapy monitoring and recurrence detection, improving patient outcomes. The comparative study of custom CNNs for brain tumour detection reveals significant advancements in the field, driven by innovative architectures, multimodal data integration, and advanced techniques. Research and development in neuro-oncology have the potential to improve diagnostic efficacy and precision despite ongoing challenges, which will ultimately result in better patient care. The potential for brain tumours to spread and result in severe neurological consequences makes them a challenging issue in the current healthcare system, endangering the lives of patients. Brain tumours are automatically classified using machine learning models such as Weiner and median filtering employed by [36] for noise removal. The image was extracted by Two-Dimensional Discrete Wavelet Transform (2D-DWT) and classified using an Artificial Neural Network (ANN) into Glioma (GL), Meningioma (MG), and Pituitary tumour (PT). The neural network resulted in an average accuracy of ACC 91.9%, [37] determined a region of interest by morphological operation after removing noise with a median filter.

A Support Vector Machine (SVM) is used in the research [38] to classify brain tumours as benign or malignant. The image features were extracted and segmented using wavelets and thresholding, respectively. The proposed SVM obtained an accuracy of 92%. The resulting images were classified into Astrocytoma, Glioblastoma, and Oligodendroglioma using the K-Nearest Neighbour Algorithm (KNN). The proposed KNN achieved an accuracy of 89.5%. The study of [39] demonstrated an improved BRATS dataset and used the Gray-Level Co-Occurrence Matrix (GLCM) to extract the features. The recovered features were classified as benign or malignant using SVM. The proposed categorisation method proved effective at 76% sensitivity, 60% specificity, and 85% accuracy. The study in [40] evaluated the degree to which brain cancers could be categorised into three groups using RELM3: pituitary, glioma, and meningioma. The classification approach worked as expected, with an accuracy of 94.25%.

As an alternative to machine learning, deep learning is frequently used to automatically extract and identify features from brain tumours. CNNs can increase the effectiveness and precision of brain tumour detection from MRI scans, as shown by prior research on deep learning for medical image categorisation. Different performance levels of tumours can be classified using CNN-based models [41], [42]. The research [28] applied normalisation, resizing, and augmentation to preprocess brain tumour images and classified them using custom CNN models for meningioma, glioma, and pituitary. In that order, the projected CNN model's accuracy, precision, and F1-score were 94.81%, 94.94%, and 91.9%. As per reference [43], Generative adversarial networks (GAN) augmentation enhanced the number of datasets. The brain tumour images were used to identify the following subtypes of glioma: IDH1 wild-type, which had mean SPE 92.17%, mean ACC 88.82%, and mean SPE 81.81%; and Isocitrate dehydrogenase one mutant (IDH1), which [44] used a pre-trained CNN called CapsulNet. The CNN model obtained a 94% F1 Score [4] and employed a custom CNN to classify brain tumours into Normal, Metastatic, Meningioma, Glioma, and Pituitary, with an accuracy of 92.66% [45]. The preprocessing steps included cropping, padding, resizing, and normalisation. The brain tumour was then classified into Grade II and Grade III using VGG16. The classification model achieved 89% accuracy, 87% sensitivity, and 92% specificity.

The reviewed studies demonstrate significant advances in brain tumour classification. In spite of all the progress achieved, there are still some challenges which prevent the development of reliable algorithms [28]– [45]. There is an inherent limited capability of CNN models to extract highly discriminative feature representation of MRI images [28], [42], [44]. While deep convolutional neural networks make automated feature extraction more effective, those algorithms could not maintain highly specific spatial features which differentiate tumours of similar radiological appearance. Another problem which remains unsolved is the issue of model generalization. Most methods used for this purpose are validated via benchmarking on individual datasets in a controlled experimental setting. The performance of those models varies significantly depending on the type of the tumour. Tumour morphology, image acquisition protocol, MRI scanner specifics, and imbalanced distribution of classes hinder the consistency of the classification process [30], [32], [43]. In addition, any improvement in prediction accuracy is often accompanied by even more complicated architectures of the neural networks, multimodal fusions, and computationally expensive learning mechanisms. Although the approach helps to improve the quality of feature learning, it increases costs of both training and inference, thus, making its application in resource-limited medical settings difficult [28], [30] [32]. Therefore, there is a need for developing a deep learning approach that learns more informative feature representations and demonstrate high-quality multiclass classification performance using heterogeneous data from MRI images.

3.0 Methodology

The computer-aided classification system for classifying brain tumours consists of data acquisition, preprocessing, model architecture design, model training, and evaluation. Gliomas, meningiomas, no tumours, and pituitaries are the four classes automatically classified using CNNs.

3.1 Data Collection

4400 MRI brain images were obtained from Kaggle [47]. The sample brain tumour dataset is shown in Figure 1. It is divided into four categories: pituitary, meningioma, glioma, and no tumour. 400 (100 for each class) were used for testing, and 4000 (1000 for each class) were used for training.

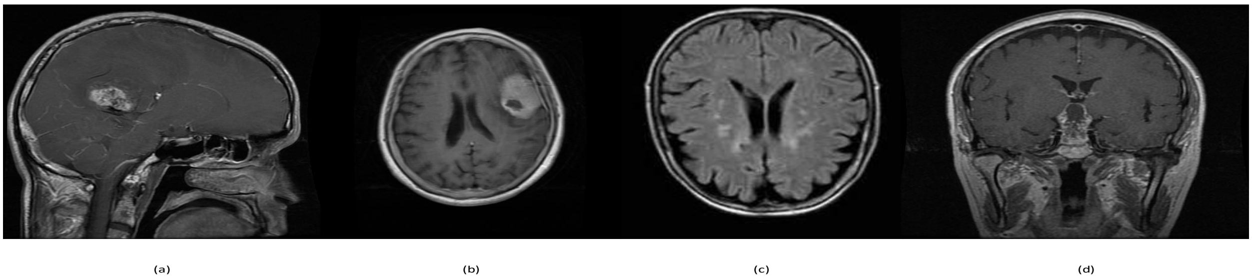

Figure 1: Sample MRI Brain Tumor images (a) Glioma (b) Meningioma (c) No tumour (d) Pituitary

3.2 Proposed DSAF-Net for Multiclass Brain Tumor Classification

Figure 2 presents the architecture of the proposed Dynamic Scale-Aware Attention Fusion Network (DSAF-Net) developed for automated multiclass brain tumor classification from magnetic resonance imaging (MRI) scans. The architecture is a sequential processing pipeline consisting of preprocessing, feature extraction, adaptive feature learning, attention enhancement, feature fusion, and final classification stages. The design combines multi-scale representation learning with adaptive attention-guided feature fusion. The network receives an MRI brain image of size 224 × 224 × 3 as input.

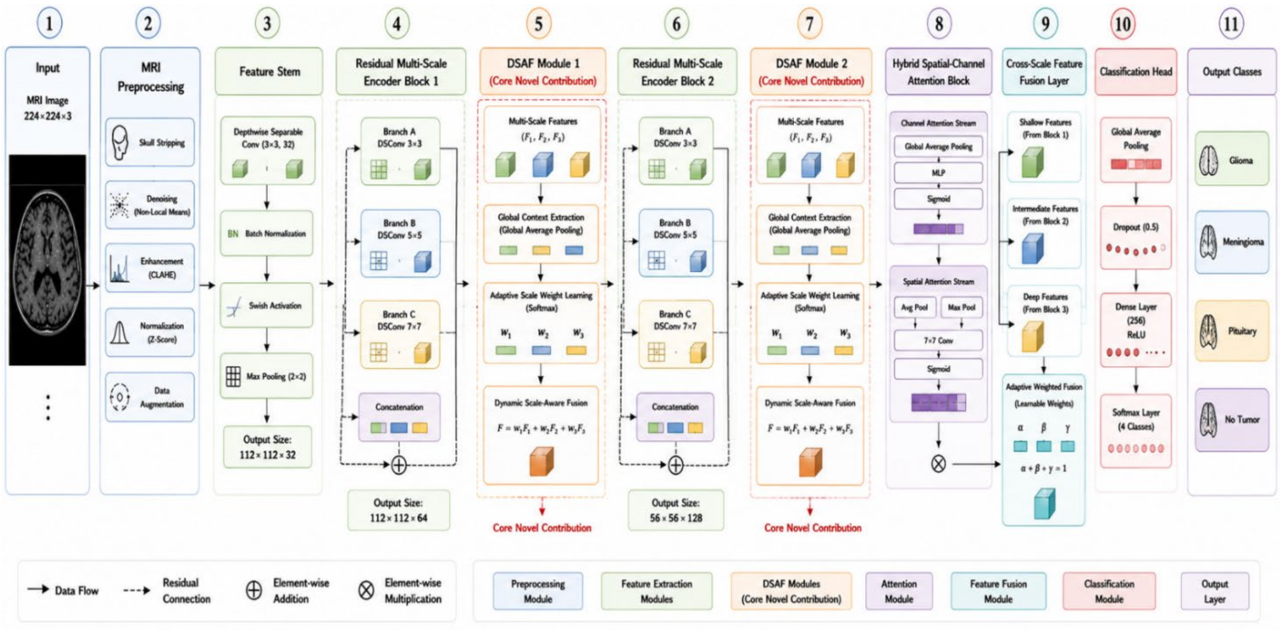

Figure 2. Architecture of the Proposed DSAF-Net for Multiclass Brain Tumor Classification

Before feature extraction, the images were preprocessed using skull stripping, Non-Local Means (NLM) denoising, contrast-limited adaptive histogram equalization (CLAHE), z-score normalization, and data augmentation. Skull stripping was performed to isolate the brain region from surrounding tissues [48]. Unlike conventional filtering techniques that rely solely on local neighborhoods. NLM denoising exploits the redundancy of similar image patches throughout the image [49]. Contrast-Limited Adaptive Histogram Equalization (CLAHE) was applied following denoising to enhance local contrast and improve the visibility of tumor regions [50]. MRI images acquired from different scanners protocols often exhibit intensity variations. Such inconsistencies can negatively affect the learning process and reduce model generalization. To address this challenge, z-score normalization was performed to standardize image intensities across the dataset [51]. The augmentation of the images was done using random rotations, horizontal flipping, zooming, translation, and minor geometric transformations [52].

Following preprocessing, the enhanced image was passed to the feature stem module. This stage consists of a depthwise separable convolution layer with a 3 × 3 kernel and 32 filters, followed by batch normalization, Swish activation, and max-pooling. The feature stem extracts fundamental low-level representations while maintaining computational efficiency through the use of depthwise separable convolutions. The extracted features were processed by the first Residual Multi-Scale Encoder Block. This block contains three parallel convolutional branches with receptive fields of different sizes, namely 3 × 3, 5 × 5, and 7 × 7. The parallel branches allow the network to capture fine-grained textures, intermediate structures, and broader contextual information simultaneously. The resulting feature maps are concatenated and integrated through a residual shortcut

Received: 04/07/2026; Revised:13/07/2026; Accepted: 16/07/2026; Published: 21/08/2026

connection, which facilitates stable gradient propagation and mitigates information loss during deep feature learning.

The first Dynamic Scale-Aware Attention Fusion (DSAF) module constitutes the primary methodological contribution of the proposed architecture. Within this module, features extracted from different receptive fields are first subjected to global context extraction through global average pooling. The resulting global descriptors are then used to learn adaptive scale weights that quantify the relative importance of each feature scale. These weights perform dynamic scale-aware fusion, enabling the network to emphasize the most informative tumor characteristics while suppressing less relevant feature responses. Unlike conventional multi-scale architectures that combine features using fixed concatenation or summation strategies, the DSAF module performs adaptive scale selection based on image content.

The refined feature representations are then processed by a second Residual Multi-Scale Encoder Block that follows a similar structure but operates at a deeper representational level. This block again employs three parallel depthwise separable convolution branches with different receptive fields and incorporates residual learning to preserve information flow throughout the network. The output is subsequently passed through a second DSAF module, allowing adaptive scale selection to be performed at multiple levels of abstraction.

After dynamic feature fusion, the architecture applies a Hybrid Spatial-Channel Attention Block to further refine the learned representations. This component consists of two complementary attention streams. The channel attention stream utilizes global average pooling followed by a multilayer perceptron and sigmoid activation to identify the most informative feature channels. In parallel, the spatial attention stream employs average pooling, max pooling, and a 7×7 convolution operation to identify diagnostically important spatial regions. The outputs of the two streams are combined through element-wise multiplication to produce attention-enhanced feature maps.

The attention-refined features are supplied to the Cross-Scale Feature Fusion Layer. This module receives feature representations originating from shallow, intermediate, and deep network stages. Through adaptive weighted fusion, the model integrates complementary information from multiple depths, thereby preserving both local texture details and high-level semantic information. This strategy enables the network to construct a richer and more discriminative representation of brain tumors.

The fused feature maps were passed to the classification head. The global average pooling transformed the spatial feature maps into a compact feature vector and reduced the number of trainable parameters. A dropout layer with a rate of 0.5 was applied to improve generalization and reduce overfitting. The resulting features were processed by a fully connected layer containing 256 neurons and ReLU activation, followed by a Softmax classifier that produced class probabilities for the four target categories. The final output layer generated predictions corresponding to four brain MRI classes: Glioma, Meningioma, Pituitary Tumor, and No Tumor. These categories represent the multiclass classification objective of the proposed framework. A notable aspect of the architecture is the visual emphasis placed on the DSAF modules. These modules are highlighted as the core novel contribution of DSAF-Net because they introduce adaptive scale-aware feature weighting and fusion, enabling the network to learn scale-specific tumor representations dynamically. This capability directly addresses the challenge of heterogeneous tumor morphology and forms the foundation of the proposed framework's discriminative power.

3.3 Model training and validation

Prior to training, the dataset was randomly divided into training, validation, and testing subsets to ensure an unbiased assessment of model performance. Table 1 presents the Training hyperparameters of the proposed model. Training was performed using mini-batch gradient optimisation with a batch size of 32. During each epoch, batches of MRI images were propagated through the network, and the corresponding prediction errors were computed using the categorical cross-entropy loss function. The learning process was further stabilised through the incorporation of batch normalisation layers. Swish activation functions. Validation performance was continuously monitored after each training epoch. A ReduceLROnPlateau scheduling strategy was employed to adaptively adjust the learning rate whenever validation improvement stagnated.

Table 1: Training Hyperparameters of the proposed model

Hyperparameter	Value
Input Image Size	$224 \times 224 \times 3$
Batch Size	32
Number of Epochs	100
Optimizer	AdamW
Initial Learning Rate	0.001
Weight Decay	1×10^{-4}
Learning Rate Sceduler	ReduceLROnPlateau
LR Reduction Factor	0.1

Hyperparameter	Value
Patience	10 Epochs
Minimum Learning Rate	1×10^{-6}
Loss Function	Categorical Cross-Entropy
Output Activation	Softmax
Hidden Layer Activation	Swish
Dropout Rate	0.5
Batch Normalization	Applied After Convolution Layers
Early Stopping	Enabled
Early Stopping Patience	15 Epochs
Data Augmentation	Enabled
Weight Initialization	He Normal
Training Platform	TensorFlow/Keras

3.4 Model Evaluation

The models' performance was evaluated using accuracy, precision, recall, F1 Score, and AUC. Accuracy (ACC) is the ratio of correctly classified images to the total number of images [53].

$$Accuracy = \frac{TP + TN}{TP + TN + FP + FN} \quad (1)$$

The precision (PRE) defines the percentage of true positive classifications among all optimistic predictions [54].

$$Precision = \frac{TP}{T\ P + FP} \quad (2)$$

Recall, also called sensitivity (SEN), provides the number of true positive classifications out of all actual positives [55].

$$Recall = \frac{TP}{TP + FN} \quad (3)$$

The $F1_{score}$ is a single statistic that balances both metrics, the harmonic average of sensitivity and precision [56].

$$F1 - score = \frac{2 \times Precision\ \times Recall}{Precision + Recall} \quad (4)$$

TP, FP, TN, and FN represent true positives, false positive, and false negatives respectively

AUC refers to the class differentiation capabilities of the model with different threshold values [57].

4.0 Results and Discussions

The results presented in the Table 2 and Figure 3 show the superior classification capability of the proposed DSAF-Net when compared with SqueezeNet, DenseNet121, and EfficientNet-B7. The three models are widely adopted deep learning architectures. Performance was evaluated using five standard classification metrics, including accuracy, precision, recall, F1-score, and AUC.

Table 2: Performance comparison of baseline models

Model	Accuracy (%)	Precision (%)	Recall (%)	F1-Score (%)	AUC (%)
SqueezeNet	96.13	95.84	95.72	95.78	98.41
DenseNet121	96.72	96.48	96.31	96.39	98.76
EfficientNet-B7	97.58	97.34	97.21	97.27	99.11
Proposed DSAF-Net	**98.94**	**98.87**	**98.76**	**98.81**	**99.72**

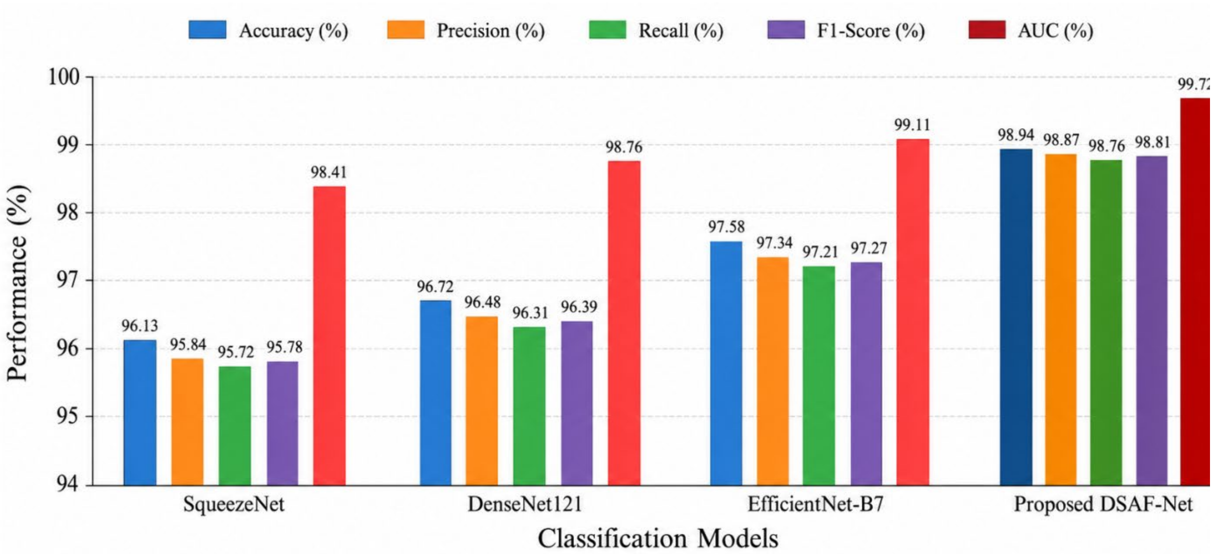

Figure 3: Visual Performance Comparison of the Proposed Model

Among all competing models, DSAF-Net achieved the highest classification accuracy of 98.94%, outperforming SqueezeNet, DenseNet121, and EfficientNet-B7 by margins of 2.81%, 2.22%, and 1.36%, respectively. The visual presentation in Figure 3 also reveals a consistent upward trend across all performance metrics as model complexity and feature representation capability increase. This improvement indicates that the proposed architecture can more effectively distinguish between the different brain tumor categories while minimizing overall classification errors. Although EfficientNet-B7 demonstrated strong performance with an accuracy of 97.58%, the proposed model consistently maintained a clear advantage across all evaluation metrics.

A similar trend can be observed in terms of precision. DSAF-Net attained a precision score of 98.87%, which reflects its ability to generate highly reliable predictions with very few false-positive classifications. In contrast, SqueezeNet, DenseNet121, and EfficientNet-B7 achieved precision values of 95.84%, 96.48%, and 97.34%, respectively. The improvement in precision suggests that the proposed feature extraction and attention mechanisms enhance class discrimination, leading to more confident and accurate predictions.

DSAF-Net obtained a recall of 98.76%, which indicates its strong capability to correctly identify tumor instances across all classes. Compared with the recall scores of 95.72% for SqueezeNet, 96.31% for DenseNet121, and 97.21% for EfficientNet-B7, the proposed model demonstrates a reduced likelihood of missing clinically important tumor cases. This characteristic is particularly valuable in medical image analysis, where false negatives can have serious diagnostic consequences. The F1-score, reached 98.81% for DSAF-Net. This represents the best overall classification balance among the evaluated models. The F1-scores obtained by SqueezeNet (95.78%), DenseNet121 (96.39%), and EfficientNet-B7 (97.27%) were consistently lower, highlighting the effectiveness of the proposed architecture in maintaining both sensitivity and prediction reliability simultaneously. DSAF-Net achieved an outstanding AUC value of 99.72%, indicating near-perfect separability among the tumor classes.

Table 3 presents the ablation study conducted to evaluate the contribution of each major component incorporated into the proposed DSAF-Net architecture. The baseline CNN achieved an accuracy of 95.21%, serving as the reference model for subsequent comparisons. Introducing residual learning improved the classification accuracy to 96.37%. This demonstrates the effectiveness of residual connections in facilitating feature propagation and improving optimization stability.

Table 3: Ablation Study of the Model Components

Model Configuration	**Accuracy (%)**	**Precision (%)**	**Recall (%)**	**1-Score (%)**	**UC (%)**
Baseline CNN	95.21	95.03	4.88	94.95	7.84
Baseline CNN + Residual Learning	96.37	96.15	96.02	96.08	8.42
Baseline CNN + Residual Learning + Multi-Scale Feature Extraction	97.26	97.11	96.95	97.03	8.87
Baseline CNN + Residual Learning + Multi-Scale Feature Extraction + Hybrid Spatial-Channel Attention	98.11	97.98	7.84	97.91	9.23

Model Configuration	Accuracy (%)	Precision (%)	Recall (%)	1-Score (%)	UC (%)
Baseline CNN + Residual Learning + Multi-Scale Feature Extraction + Hybrid Attention + Cross-Scale Feature Fusion	98.56	98.41	98.29	98.35	9.51
Proposed DSAF-Net (Full Model)	**98.94**	**98.87**	**8.76**	**98.81**	**9.72**

The incorporation of multi-scale feature extraction further increased the accuracy to 97.26%, indicating that the simultaneous extraction of features at different receptive fields enhances the model's ability to capture diverse tumor characteristics. Adding the Hybrid Spatial-Channel Attention mechanism resulted in an accuracy of 98.11%, highlighting the importance of selectively emphasizing discriminative tumor features while suppressing irrelevant background information. The integration of the Cross-Scale Feature Fusion strategy produced an additional performance gain, increasing the accuracy to 98.56%. This improvement confirms that combining shallow, intermediate, and deep feature representations provides complementary information for tumor classification. The complete DSAF-Net architecture, incorporating the proposed Dynamic Scale-Aware Attention Fusion module, achieved the highest performance across all evaluation metrics, reaching an accuracy of 98.94% and an AUC of 99.72%. These results demonstrate that each component contributes positively to the overall classification performance, while the proposed DSAF module provides the largest improvement by enabling adaptive scale selection and dynamic feature fusion for heterogeneous brain tumor representations.

5.0 Practical Implications for clinical decision-support systems

The high classification accuracy achieved by the proposed DSAF-Net demonstrates its potential to assist radiologists and medical practitioners in the rapid and reliable interpretation of brain MRI scans. By automatically distinguishing among glioma, meningioma, pituitary tumour, and normal brain images, the framework can serve as an auxiliary diagnostic tool that supports clinical assessment and reduces the workload associated with manual image analysis. The integration of dynamic scale-aware feature fusion and hybrid attention mechanisms enables the model to identify subtle tumour characteristics that may be difficult to detect consistently through visual inspection alone. This capability may contribute to improved diagnostic consistency, particularly in high-volume healthcare environments where radiologists are required to evaluate large numbers of imaging studies within limited timeframes. Consequently, the proposed system has the potential to reduce diagnostic variability and support more informed clinical decision-making.

Another practical advantage of the proposed framework is its computational efficiency relative to much large-scale deep learning architecture. The use of depthwise separable convolutions, residual learning, and adaptive feature fusion allows the network to achieve high classification performance while maintaining a manageable computational burden. This characteristic increases the feasibility of deploying the system in hospitals, diagnostic centres, and healthcare facilities where computing resources may be limited. Furthermore, the proposed model may be integrated into computer-aided diagnosis platforms to provide real-time tumour classification during routine MRI examinations. Such integration could facilitate earlier detection of abnormal findings, accelerate patient referral processes, and support treatment planning by providing clinicians with an additional source of diagnostic information. In regions where access to experienced radiologists is limited, automated classification systems could also contribute to improving the accessibility and quality of healthcare services.

6.0 Limitations of the Proposed System

Despite the promising performance achieved by the proposed Dynamic Scale-Aware Attention Fusion Network (DSAF-Net), several limitations should be acknowledged. The proposed framework relies exclusively on structural MRI images for tumour classification. In clinical practice, radiologists often utilise additional imaging modalities and patient-specific information to support diagnosis. The absence of such complementary information may limit the model's ability to capture the complete clinical characteristics of certain tumour types. Another limitation relates to model interpretability. Like many deep learning approaches, DSAF-Net functions primarily as a data-driven predictive system, and its internal decision-making process may not always be fully transparent to clinicians. Although the incorporated attention mechanisms provide some insight into salient image regions, further explainability techniques such as Gradient-weighted Class Activation Mapping (Grad-CAM) and explainable artificial intelligence (XAI) frameworks could enhance clinical trust and facilitate adoption.

7.0 Conclusion and Future Work

This study presented DSAF-Net, a novel Dynamic Scale-Aware Attention Fusion Network for multiclass brain tumour classification using MRI images. The proposed network architecture was designed to overcome some existing problems associated with current deep learning models, such as poor feature representation, limited

Received: 04/07/2026; Revised:13/07/2026; Accepted: 16/07/2026; Published: 21/08/2026

discrimination between tumour subtypes. To overcome these limitations, DSAF-Net integrates residual multi-scale feature extraction, dynamic scale-aware attention fusion, hybrid spatial-channel attention, and cross-scale feature aggregation within a unified deep learning framework. Experimental evaluation was conducted on a publicly available brain MRI dataset comprising four categories. The results demonstrated the effectiveness of the proposed architecture, achieving an overall classification accuracy of 98.94%, precision of 98.87%, recall of 98.76%, F1-score of 98.81%, and an AUC of 99.72%. Comparative analysis further revealed that DSAF-Net consistently outperformed several established deep learning models, including SqueezeNet, DenseNet121, and EfficientNet-B7. The ablation study also confirmed the positive contribution of each architectural component, with the Dynamic Scale-Aware Attention Fusion module providing the most substantial performance improvement. These findings indicate that adaptive multi-scale representation learning plays a critical role in capturing the heterogeneous characteristics of brain tumours and improving classification reliability.

Despite these outcomes, several opportunities remain for further investigation. Future work can focus on validating the proposed framework using larger multi-institutional datasets collected from different imaging centres. The incorporation of multimodal imaging information may further enhance diagnostic performance by providing complementary tumour characteristics. Similarly, extending the framework to support tumour segmentation, grading, and prognosis prediction could broaden its applicability within comprehensive neuro-oncological decision-support systems.

References

[1] C. McNamara *et al.*, “2021 WHO classification of tumours of the central nervous system: a review for the neuroradiologist,” *Neuroradiology*, vol. 64, no. 10, pp. 1919–1950, 2022.

[2] D. N. Louis *et al.*, “I nternational S ociety of N europathology-H aarlem C onsensus G uidelines for N ervous S ystem T umor C lassification and G rading,” *Brain Pathol.*, vol. 24, no. 5, pp. 429–435, 2014.

[3] Y. Bhanothu, A. Kamalakannan, and G. Rajamanickam, “Detection and classification of brain tumor in MRI images using deep convolutional network,” in *2020 6th international conference on advanced computing and communication systems (ICACCS)*, 2020, pp. 248–252.

[4] E. Irmak, “Multi-classification of brain tumor MRI images using deep convolutional neural network with fully optimised framework,” *Iran. J. Sci. Technol. Trans. Electr. Eng.*, vol. 45, no. 3, pp. 1015–1036, 2021.

[5] Ö. Polat and C. Güngen, “Classification of brain tumors from MR images using deep transfer learning,” *J. Supercomput.*, vol. 77, no. 7, pp. 7236–7252, 2021.

[6] A. Işın, C. Direkoğlu, and M. Şah, “Review of MRI-based brain tumor image segmentation using deep learning methods,” *Procedia Comput. Sci.*, vol. 102, pp. 317–324, 2016.

[7] J. Potočnik, E. Thomas, R. Killeen, S. Foley, A. Lawlor, and J. Stowe, “Automated vetting of radiology referrals: exploring natural language processing and traditional machine learning approaches,” *Insights Imaging*, vol. 13, no. 1, pp. 1–8, 2022.

[8] O. A. Adebisi, J. A. Ojo, and O. M. Oni, “Comparative analysis of deep learning models for detection of COVID-19 from chest X-Ray images,” *Int. J. Sci. Res. Comput. Sci. Eng. Vol*, vol. 8, no. 5, 2020.

[9] N. Kesav and M. G. Jibukumar, “Efficient and low complex architecture for detection and classification of Brain Tumor using RCNN with Two Channel CNN,” *J. King Saud Univ. Inf. Sci.*, vol. 34, no. 8, pp. 6229–6242, 2022.

[10] O. A. Adebisi, O. Busari, Y. Oyewola, and I. Adeaga, “Automatic classification of lung nodules on computed tomography images using a pre-trained convolutional neural network,” *Int. J. Eng. Sci. Invent.*, vol. 9, no. 1, pp. 63–66, 2020.

[11] S. M. Anwar, M. Majid, A. Qayyum, M. Awais, M. Alnowami, and M. K. Khan, “Medical image analysis using convolutional neural networks: a review,” *J. Med. Syst.*, vol. 42, pp. 1–13, 2018.

[12] G. Gokulkumari, “Classification of brain tumor using manta ray foraging optimisation-based DeepCNN classifier,” *Multimed. Res.*, vol. 3, no. 4, pp. 32–42, 2020.

[13] P. Nagaraj, V. Muneeswaran, L. V. Reddy, P. Upendra, and M. V. V. Reddy, “Programmed multi-classification of brain tumor images using deep neural network,” in *2020 4th international conference on intelligent computing and control systems (ICICCS)*, 2020, pp. 865–870.

[14] A. Hosny, C. Parmar, J. Quackenbush, L. H. Schwartz, and H. J. W. L. Aerts, “Artificial intelligence in radiology,” *Nat. Rev. Cancer*, vol. 18, no. 8, pp. 500–510, 2018.

[15] R. Mehrotra, M. A. Ansari, R. Agrawal, and R. S. Anand, “A transfer learning approach for AI-based classification of brain tumors,” *Mach. Learn. with Appl.*, vol. 2, p. 100003, 2020.

[16] S. Özen, “Süperiletkenlerde kaldırma kuvvetinin incelenmesi.” Niğde Ömer Halisdemir Üniversitesi/Fen Bilimleri Enstitüsü, 2019.

[17] M. A. Mazurowski, H. Dong, H. Gu, J. Yang, N. Konz, and Y. Zhang, “Segment anything model for medical image analysis: an experimental study,” *Med. Image Anal.*, vol. 89, p. 102918, 2023.

[18] M. Puttagunta and S. Ravi, “Medical image analysis based on deep learning approach,” *Multimed. Tools Appl.*,

vol. 80, pp. 24365–24398, 2021.

[19] V. D. P. Jasti *et al.*, "Computational technique based on machine learning and image processing for medical image analysis of breast cancer diagnosis," *Secur. Commun. networks*, vol. 2022, pp. 1–7, 2022.

[20] C. Parmar, J. D. Barry, A. Hosny, J. Quackenbush, and H. J. W. L. Aerts, "Data analysis strategies in medical imaging," *Clin. cancer Res.*, vol. 24, no. 15, pp. 3492–3499, 2018.

[21] R. B. Jeyavathana, R. Balasubramanian, and A. A. Pandian, "A survey: analysis on preprocessing and segmentation techniques for medical images," *Int. J. Res. Sci. Innov.*, vol. 3, no. 6, pp. 113–120, 2016.

[22] P. O. Adejumobi, I. O. Adejumobi, O. A. Adebisi, S. O. Ayanlade, and I. I. Adeaga, "Automatic Classification of Breeds of Dog using Convolutional Neural Network," *Niger. J. Technol. Dev.*, vol. 20, no. 3, 2023.

[23] N. Tajbakhsh *et al.*, "Convolutional neural networks for medical image analysis: Full training or fine tuning?," *IEEE Trans. Med. Imaging*, vol. 35, no. 5, pp. 1299–1312, 2016.

[24] O. A. Adebisi, J. A. Ojo, and T. O. Bello, "Computer-aided diagnosis system for classification of abnormalities in thyroid nodules ultrasound images using deep learning," *IOSR J. Comput. Eng.*, vol. 22, no. 3, pp. 60–66, 2020.

[25] D. Shen, G. Wu, and H.-I. Suk, "Deep learning in medical image analysis," *Annu. Rev. Biomed. Eng.*, vol. 19, pp. 221–248, 2017.

[26] O. A. Adebisi, S. A. Ajagbe, J. A. Ojo, and M. A. Oladipupo, "Computer Techniques for Medical Image Classification: A Review," *Intell. Healthc. Infrastructure, Algorithms Manag.*, pp. 19–36, 2022.

[27] M. De Bruijne, "Machine learning approaches in medical image analysis: From detection to diagnosis," *Medical image analysis*, vol. 33. Elsevier, pp. 94–97, 2016.

[28] M. M. Badža and M. Č. Barjaktarović, "Classification of brain tumors from MRI images using a convolutional neural network," *Appl. Sci.*, vol. 10, no. 6, p. 1999, 2020.

[29] D. Goyal and H. Sharma, "Brain Tumor Detection System Using Neural Networks," *Int. J. Commun. Inf. Technol.*, vol. 4, no. 1, pp. 59–63, 2023,. DIO: 10.33545/2707661X.2023.V4.I1A.61

[30] V. N. V. L. S. Swathi, "Deep Learning-Based Brain Tumor Detection: An MRI Segmentation Approach," *Matec Web Conf.*, vol. 392, p. 1157, 2024,. DIO: 10.1051/MATECCONF/202439201157

[31] M. Thorat, "Automated Brain Tumor Detection Using Deep Learning and Flask Web Application," *Asian J. Converg. Technol.*, vol. 10, no. 1, pp. 69–73, 2024,. DIO: 10.33130/AJCT.2024V10I01.014

[32] M. Hammad, M. ElAffendi, A. A. Ateya, and A. A. A. El-Latif, "Efficient Brain Tumor Detection With Lightweight End-to-End Deep Learning Model," *Cancers (Basel).*, vol. 15, no. 10, p. 2837, 2023,. DIO: 10.3390/CANCERS15102837

[33] H. Alsaif *et al.*, "A Novel Data Augmentation-Based Brain Tumor Detection Using Convolutional Neural Network," *Appl. Sci.*, vol. 12, no. 8, p. 3773, 2022,. DIO: 10.3390/APP12083773

[34] V. Anand *et al.*, "Weighted Average Ensemble Deep Learning Model for Stratification of Brain Tumor in MRI Images," *Diagnostics*, vol. 13, no. 7, p. 1320, 2023,. DIO: 10.3390/DIAGNOSTICS13071320

[35] A. Stadlbauer *et al.*, "Radiophysiomics: Brain Tumors Classification by Machine Learning and Physiological MRI Data," *Cancers (Basel).*, vol. 14, no. 10, p. 2363, 2022,. DIO: 10.3390/CANCERS14102363

[36] C. R. Park, S.-H. Kang, and Y. Lee, "Median modified wiener filter for improving the image quality of gamma camera images," *Nucl. Eng. Technol.*, vol. 52, no. 10, pp. 2328–2333, 2020.

[37] R. H. Ramdlon, E. M. Kusumaningtyas, and T. Karlita, "Brain tumor classification using MRI images with K-nearest neighbor method," in *2019 International Electronics Symposium (IES)*, 2019, pp. 660–667.

[38] M. Gurbină, M. Lascu, and D. Lascu, "Tumor detection and classification of MRI brain image using different wavelet transforms and support vector machines," in *2019 42nd International Conference on Telecommunications and Signal Processing (TSP)*, 2019, pp. 505–508.

[39] V. Wasule and P. Sonar, "Classification of brain MRI using SVM and KNN classifier," in *2017 third international conference on sensing, signal processing and security (ICSSS)*, 2017, pp. 218–223.

[40] A. Gumaei, M. M. Hassan, M. R. Hassan, A. Alelaiwi, and G. Fortino, "A hybrid feature extraction method with regularised extreme learning machine for brain tumor classification," *IEEE Access*, vol. 7, pp. 36266–36273, 2019.

[41] M. Havaei *et al.*, "Brain tumor segmentation with deep neural networks," *Med. Image Anal.*, vol. 35, pp. 18–31, 2017.

[42] O. Adeyemi, I. A. Ayoade, E. O. Adeyemi, O. O. Olanrele, I. Eweoya, and J. Matthew, "Adoption of artificial intelligence in operations management: A design-oriented review," in *Advances in Manufacturing Technology-XXXVII: Proceedings from the 20th International Conference on Manufacturing Research*, 2023, pp. 17–23.

[43] C. Ge, I. Y.-H. Gu, A. S. Jakola, and J. Yang, "Enlarged training dataset by pairwise GANs for molecular-based brain tumor classification," *IEEE access*, vol. 8, pp. 22560–22570, 2020.

[44] R. Vimal Kurup, V. Sowmya, and K. P. Soman, "Effect of data preprocessing on brain tumor classification using capsulenet," in *ICICCT 2019–System reliability, quality control, safety, maintenance and management: Applications to electrical, electronics and computer science and engineering*, 2020, pp. 110–119.

Received: 04/07/2026; Revised:13/07/2026; Accepted: 16/07/2026; Published: 21/08/2026

[45] M. A. Naser and M. J. Deen, "Brain tumor segmentation and grading of lower-grade glioma using deep learning in MRI images," *Comput. Biol. Med.*, vol. 121, p. 103758, 2020.

[46] M. Prastawa, E. Bullitt, N. Moon, K. Van Leemput, and G. Gerig, "Automatic brain tumor segmentation by subject specific modification of atlas priors1," *Acad. Radiol.*, vol. 10, no. 12, pp. 1341–1348, 2003.

[47] M. Nickparvar, "Brain Tumor MRI Dataset." [Online]. Available: https://www.kaggle.com/datasets/masoudnickparvar/brain-tumor-mri-dataset

[48] P. Kalavathi and V. S. Prasath, "Methods on skull stripping of MRI head scan images—A review," IEEE J. Digit. Imaging, vol. 29, no. 3, pp. 365–379, Jun. 2016.

[49] J. V. Manjón, J. Carbonell-Caballero, J. J. Lull, G. García-Martí, L. Martí-Bonmatí, and M. Robles, "MRI denoising using non-local means," Med. Image Anal., vol. 12, no. 4, pp. 514–523, Aug. 2008.

[50] K. Zuiderveld, "Contrast limited adaptive histogram equalization," in Graphics Gems IV, P. S. Heckbert, Ed. San Diego, CA, USA: Academic Press Professional, 1994, pp. 474–485.

[51] K. Cabello-Solorzano, I. Ortigosa de Araujo, M. Peña, L. Correia, and A. J. Tallón-Ballesteros, "The impact of data normalization on the accuracy of machine learning algorithms: A comparative analysis," in Proc. Int. Conf. Soft Computing Models in Industrial and Environmental Applications, Cham, Switzerland: Springer Nature Switzerland, 2023, pp. 344–353.

[52] K. Maharana, S. Mondal, and B. Nemade, "A review: Data pre-processing and data augmentation techniques," Global Transitions Proc., vol. 3, no. 1, pp. 91–99, Jun. 2022.

[53] A. A. Adegun, S. Viriri, and J.-R. Tapamo, "Review of Deep Learning methods for remote sensing satellite images classification: experimental survey and comparative analysis," *J. Big Data*, vol. 10, no. 1, p. 93, Jun. 2023, doi: 10.1186/s40537-023-00772-x.

[54] G. Forman, "Counting Positives Accurately Despite Inaccurate Classification," 2005, pp. 564–575. doi: 10.1007/11564096_55.

[55] V. Kumar, R. K. Kumar, and S. K. Singh, "Evaluation and Enhancement of Standard Classifier Performance by Resolving Class Imbalance Issue Using Smote-Variants Over Multiple Medical Datasets," *SN Comput. Sci.*, vol. 6, no. 3, p. 286, Mar. 2025, doi: 10.1007/s42979-025-03775-y.

[56] K. M. Sujon, R. Hassan, K. Choi, and M. A. Samad, "Accuracy, precision, recall, f1-score, or MCC? empirical evidence from advanced statistics, Machine Learning and XAI for evaluating business predictive models," *J. Big Data*, vol. 12, no. 1, p. 268, Dec. 2025, doi: 10.1186/s40537-025-01313-4.

[57] J. Huang and C. X. Ling, "Using AUC and accuracy in evaluating learning algorithms," IEEE Trans. Knowl. Data Eng., vol. 17, no. 3, pp. 299–310, Mar. 2005.